The Journal of Neuroscience, May 1994, 14(5): 3319–3332

Properties of "Reconstructed" Motor Synapses of the Garter Snake

R. S. Wilkinson and S. D. Lunin

Department of Cell Biology and Physiology, Washington University School of Medicine, St. Louis, Missouri 63110

We have developed a technique, called synaptic reconstruction, that permits nerve terminals of living vertebrate neuromuscular junctions (NMJs) to be isolated and then manually recombined with vacant endplate sites to form functional synapses. By reconstructing NMJs with various combinations of pre- and postsynaptic partners, or with varying degrees of pre- to postsynaptic alignment, the functional properties of the three anatomical components of the NMJ—nerve terminal, endplate, and the alignment between them—may be studied independently. Our experiments thus far indicate, surprisingly, that reconstructed NMJs function nearly normally. Thus, one feature of the intact vertebrate NMJ, precise alignment between presynaptic active zones and postsynaptic secondary folds, is either unnecessary for normal function or, alternatively, is spontaneously reestablished when an isolated terminal and vacant endplate site are placed in contact. We have also utilized synaptic reconstruction to examine a recently described property of NMJs: the regulation of quantal size among motor synapses in one muscle so that larger muscle fibers receive larger single quantal currents. Quantal size appears to be a postsynaptic attribute, suggesting that its regulation is achieved by a postsynaptic mechanism.

[Key words: neuromuscular junction, synapse, quantal content, nerve terminal, synaptic structure and function]

Chemical synapses comprise three structural components: the presynaptic terminal, the postsynaptic receptor site, and the spatial relationship in which the pre- and postsynaptic partners are disposed. Although anatomically discrete, the three components interact functionally and, particularly at fast synapses, they are closely opposed. These characteristics have made it difficult to study behavior of synaptic components independently in order to determine which component is associated with a particular synaptic function, or vice versa. The complex behavior of some central synapses has received attention in this regard, for example, the question of whether long-term potentiation (LTP) is initiated via pre- or postsynaptic structural modifications (see Fazeli, 1992). However, the inaccessibility of synaptic components has impeded study of more basic synaptic structure–function relationships as well, including those exhibited by the relatively simple vertebrate neuromuscular junction (NMJ).

Received Aug. 13, 1993; revised Nov. 2, 1993; accepted Nov. 24, 1993.

We thank Z. Jiang for technical assistance, P. Bridgeman and G. Phillips for expert help with electron microscopy, and J. H. Steinbach for a critical reading of the manuscript. This work was supported by NIH Grant NS 24752 and by the Muscular Dystrophy Association of America.

Correspondence should be addressed to R. S. Wilkinson, Department of Cell Biology, Washington University School of Medicine, 4566 Scott Avenue, St. Louis, MO 63110.

One key feature of the NMJ (and other synapses) is appropriate *strength,* or amount of postsynaptic conductance change associated with each action potential invading the presynaptic terminal. Ability to regulate strength dynamically is a ubiquitous synaptic function, with LTP and other well-known types of synaptic plasticity being particular cases. Thus, synaptically coupled cells throughout the nervous system are "matched"—via a variety of long- and short-term mechanisms such as synaptic growth, depression, potentiation, and facilitation—so that the strength of each synapse at a given time is appropriate to its functional role (reviewed by Grinnell and Herrera, 1981; Van der Kloot, 1991). Compelling evidence for matching (and for the regulation of synaptic strength to achieve it) comes from the adult twitch fiber NMJ: larger muscle fibers, which have higher input conductance and therefore require more current to reach threshold, receive stronger NMJs than do smaller fibers in the same muscle (Kuno et al., 1971). Moreover, the matching is regulated dynamically throughout life, because influences such as growth or atrophy of the target cell (Balice-Gordon et al., 1990) appropriately increase or decrease synaptic strength in adults.

Despite the importance of synaptic strength, little is known about the structural modifications that underlie its regulation. Either of the two determinants of strength, quantal size and quantal content, might be regulated at a particular class of synapses (see Korn and Faber, 1991). At the snake NMJ, both vary systematically with muscle fiber size (or input conductance), indicating that both are regulated (Wilkinson et al., 1992). However, neither regulatory mechanism has been successfully related to NMJ structure. Quantal content is determined, at least in part, presynaptically (i.e., the binomial number of release sites), but attempts to correlate quantal content with presynaptic structural features such as terminal area (Kuno et al., 1971; Harris and Ribchester, 1979) or estimated number of active zones (Nudell and Grinnell, 1982; Propst and Ko, 1987) have yielded poor results, with correlation coefficients in the range from 0.2 to 0.5 (see Wilkinson et al., 1992). This suggests that other factors, such as those that affect the binomial probability of release, are also involved. These unknown factors could be either presynaptic (e.g., Smith, 1991; Coniglio et al., 1993) or postsynaptic, the latter implying negative feedback from the postsynaptic cell (Bowman et al., 1989). Similarly, quantal size depends on the amount of transmitter contained in a vesicle (a presynaptic attribute) but it also depends on response properties of receptors (postsynaptic) as well as the size, shape, and contents of the synaptic cleft (alignment; quantal size reviewed by Van der Kloot, 1991). Thus, the relative importance of each of the three synaptic components in the regulation of synaptic strength (and therefore in mechanisms that underlie synaptic plasticity generally) is unclear. Indeed, multiple mechanisms within each synaptic component are potentially involved.

While synaptic strength is a functional property whose anatomical correlate is unclear, there are examples of the converse as well, namely, anatomical features of synapses with no apparent function. One is the series of postsynaptic membrane invaginations, or secondary folds, which are found precisely opposite presynaptic active zones of most vertebrate NMJs. The folds, and their alignment with active zones, have been presumed important to synaptic function, but the actual role of this striking submicrometer-level organization remains a complete mystery (see Vautrin and Mambrini, 1989).

A simple way to resolve questions such as those discussed above is direct comparison among pre- or postsynaptic components isolated from different synapses, or among one synapse's release sites and receptors configured in various orientations. However, the types of experiments possible have been limited, mostly for technical reasons. Postsynaptic sites studied after removal of their nerve terminal have provided useful information (e.g., Kuffler and Yoshikami, 1975), but in experiments where the agonist (or another drug) is applied focally, positioning of the drug-containing pipette is not sufficiently repeatable for quantitative comparisons among postsynaptic sites suspected of having different properties (but see Dionne and Liebowitz, 1982). Study of transmitter release from isolated nerve terminals, using for example outside-out patches of receptor membrane, would presumably suffer from the same problem were functional isolated nerve terminals available for study (see also Drewe et al., 1988; Girod et al., 1990). Similarly, excepting computer simulations (Bartol et al., 1991) or theoretical modeling (Vautrin and Mambrini, 1989), there has been no experimental approach available to isolate the role of pre- to postsynaptic alignment in synaptic function.

We describe here a technique that overcomes some of these experimental limitations, and thereby helps facilitate independent study of the three synaptic components. Living nerve terminals (together with their axons) are removed from endplates by a largely mechanical means that utilizes relatively little enzymatic digestion. As a result, the dissociated terminals and postsynaptic sites remain healthy for hours and can be studied in isolation. Moreover, the isolated components immediately reestablish functional synapses when terminals are micromanipulated onto either their original vacant endplate site or another vacant endplate site. As expected, properties of these "reconstructed" synapses depend on those of each synaptic partner and on the partners' relative orientation. Our studies utilizing reconstructed snake NMJs suggest that close pre- to postsynaptic spacing is essential, but raise doubts about the need for precise alignment between active zones and secondary folds in order to achieve synaptic function. In addition, by forming "mixed" synapses comprising a nerve terminal from one NMJ coupled to the endplate site of another, we have begun to compare terminals and endplate sites among different types of NMJs found in one snake muscle. We find that one functional property, regulation of quantal size, is primarily associated with the postsynaptic component.

Part of the work described has appeared in abstract form (Wilkinson and Lunin, 1991).

Materials and Methods

Adult garter snakes (*Thamnophis sirtalis*) were anesthetized by submersion in ice water (10 min) and killed by rapid decapitation. The transversus abdominis muscle was dissected from the animal and placed in a chamber containing reptilian saline solution (dissecting procedure and composition of saline in Wilkinson and Lichtman, 1985; Lichtman and Wilkinson, 1987).

Characterization of NMJs. The snake transversus abdominis muscle contains ~100 fibers of three types arranged in a predominantly single-fiber-thick sheet. The muscle is innervated exclusively on its ventral side, so that all NMJs are visible and accessible for manipulation when this side of the preparation is placed facing up in an experimental chamber (Wilkinson and Lichtman, 1985). Fibers of each type are innervated by one to four motor neurons of a corresponding type to form motor units (Lichtman and Wilkinson, 1987). Each motor unit contains 4–20 fibers that exhibit uniform contractile and metabolic properties, but vary in diameter and input conductance (Nemeth et al., 1991; Wilkinson et al., 1992). In the present study components of NMJs (terminal and endplate site) were classified with respect to the type, diameter and, in some experiments, input conductance, G_{in}, of the innervated fiber, but motor unit identity was ignored. Fiber types were assigned using anatomical criteria (Ridge, 1971; Wilkinson and Nemeth, 1989); these types correspond exactly to those determined by conventional metabolic and myosin-based typing schemes (Wilkinson et al., 1991). Briefly, faster twitch fibers (F; large diameter and similar to mammalian type IIB) were innervated at a large, solitary endplate site and lacked intracellular lipid droplets that are visible with Nomarski optics. Slower twitch fibers (S; intermediate diameter and similar to mammalian type IIA) had a large solitary endplate and contained lipid droplets. Tonic fibers (T; smallest diameter and similar to mammalian type I) were innervated at five to seven small endplate sites and contained lipid droplets. Fiber diameter was measured in the endplate region, using a calibrated eyepiece reticle. G_{in} was measured by voltage clamp using two intracellular microelectrodes placed near the endplate, roughly at the longitudinal center of the fiber, as previously described (Wilkinson et al., 1992).

Dissociation of nerve terminals from endplate sites. Our procedure was adapted from those of Kuffler and Yoshikami (1975) and Neher et al. (1978). The transversus abdominis muscle was incubated (on a shaker table at low speed) at room temperature (24°C) for 30 min in reptilian saline containing zero added Ca^{2+} and 1 mM EGTA. Reduction of Ca^{2+} levels in the bath seemed to help disrupt the muscle's connective tissue, rendering it more sensitive to subsequent enzymatic digestion (see Trube, 1983). Before or during EGTA exposure, the muscle was viewed with Nomarski optics to select and characterize appropriate terminals for dissociation (see above). Following EGTA exposure the muscle was placed on a shaker table for 15 min in reptilian saline containing 0.5 mg/ml collagenase (type I, Sigma Chemicals, St. Louis, MO) and normal (3.6 mM) Ca^{2+}, the latter to promote activity of the enzyme (Trube, 1983). The preparation was then rinsed for 30 min with several solution changes of reptilian saline containing zero added Ca^{2+}. After rinsing the preparation was transferred to an inverted microscope equipped with Nomarski optics. The ~1 ml volume of the microscope chamber was rapidly perfused with reptilian saline containing no added Ca^{2+} for the remainder of the procedure. The selected NMJ was visualized, and a pipette for local application of protease solution (tip diameter ~ 15 μm) was positioned with a micromanipulator so that it was aimed at the NMJ at roughly a 30° angle from horizontal, with its tip ~10 μm away. A glass probe (usually a patch pipette) was positioned opposite the protease-containing pipette using a second micromanipulator. Reptilian saline containing normal Ca^{2+} and 0.8 mg/ml protease (type XXV, Sigma Chemicals, St. Louis, MO) was ejected from the pipette by a syringe pump. Flow rate of the protease solution into the perfused bath was made just rapid enough (0.1–0.2 μl/sec) that the NMJ being treated was visibly "blasted" by the protease stream, as indicated by dimpling of the fiber and movement of the terminal axon branch. This rate and the rate of bath perfusion were periodically checked by ejecting a dye from the pipette to confirm localization of enzyme and Ca^{2+} to the immediate region of one NMJ. After 1–4 min of protease ejection, the glass probe was used to tug gently on the axon branch of the treated terminal until the terminal was removed from the endplate (see McMahan et al., 1972). The appropriate time to manipulate the terminal was signaled by a change in the NMJ's appearance. Nomarski contrast increased slightly, approaching the appearance of a detached terminal (see Fig. 6). Removal of the terminal ~1 min after the change of appearance was ideal. Attempting to remove the terminal slightly earlier severed the connectives to a few terminal boutons, leaving them in place on the endplate, while the rest of the terminal (20–60 boutons) and the axon were freed (see Wilkinson and Lunin, 1992). Conversely, if protease ejection was allowed to continue ~2 min or longer after the change of appearance, the terminal became dissociated without mechanical ma-

nipulation. However, the terminal was damaged, and NMJs reconstructed from the terminal were not functional. When desired, additional terminals were removed by the same procedure of protease "blasting" and mechanical tugging. After removal of the terminal(s), the preparation was rinsed in normal reptilian saline for 10–15 min before use. A rough map of the muscle showing the location of the dissociated NMJ(s) was made so that the NMJ(s) could be quickly located after the preparation was transferred to the experimental microscope (see below).

The procedure described was the most stable of several variants tried, in that satisfactory preparations were obtained >80% of the time, and minimal adjustments were required for different enzyme lots, different room temperatures, and so on. A common problem was failure to confine the protease stream to a small region of the muscle. This resulted in overall degradation of the preparation, as evidenced by spontaneous contraction of fibers and formation of "contraction clots" in fibers. The same degradation resulted if the collagenase pretreatment was prolonged, presumably due to nonspecific protease activity present in our reagent. Frequently, the protease stream affected NMJs adjacent to the chosen NMJ, as evidenced by change in their Nomarski contrast, but this seemed to be of no consequence.

Reconstruction of NMJs. Preparations with one or more detached terminals (and thus one or more vacant endplate sites) were transferred to an inverted microscope equipped with Nomarski and fluorescence optics. Both detached terminals and vacant endplate sites exhibited more Nomarski contrast than did intact NMJs and were therefore easily located (see Fig. 6). An exception was tonic fiber NMJs, which could barely be resolved over the rough, grainy appearance of lipid droplets contained within the underlying muscle fiber. When a tonic terminal was removed, its former endplate site was often invisible. For this reason, only a few tonic (T) NMJs were studied. In most experiments, twitch fiber (F or S) NMJs were reconstructed from their original synaptic partners. To do this a glass probe (a patch pipette with tip diameter of ~1 μm) was used to manipulate the terminal back onto its endplate site. A micromanipulator with low drift (MX-530, Newport Corp., Irvine, CA) was essential in order to keep the terminal in firm contact with the endplate. Drift in the downward direction damaged the terminal or the underlying muscle fiber, while drift in the upward direction resulted in cessation of synaptic function (see Results). Direct contact between the glass probe and the nerve terminal was avoided. Instead, connective tissue lying within the plane of the terminal and attached to it was pushed or pulled with the probe to guide the terminal. The connective tissue strands could rarely be visualized directly, but their presence was inferred from movement of the terminal. Reconstruction of "mixed" NMJs (those comprising a terminal and endplate that were not originally synaptic partners) was similar, except that only those endplates within range of the terminal's axon branch could be selected.

Electrophysiological recording. Miniature endplate potentials (MEPPs) and evoked endplate potentials (EPPs) or action potentials (APs) were recorded intracellularly using sharp glass micropipettes, digitized, stored on magnetic disk, and subsequently analyzed. All data were normalized to a resting potential of −80 mV and corrected for nonlinear summation. Quantal content was calculated as mean corrected EPP amplitude divided by mean corrected MEPP amplitude. Details of the recording methods and analysis of data are given elsewhere (Wilkinson et al., 1992). In a previous study of intact snake NMJs we found that miniature endplate current (MEPC) amplitudes recorded in the conventional manner using the two-electrode voltage-clamp technique corresponded well with those calculated as mean MEPP amplitude × G_{in} (Wilkinson et al., 1992). The advantage of calculating MEPCs from MEPPs is that two intracellular electrodes are needed briefly while G_{in} is measured, but only a single electrode is needed during the much longer period in which spontaneous events are recorded. To reduce possibility of impalement-related damage to muscle fibers, this technique was used in experiments where MEPCs were compared among different reconstructed NMJs. To activate nerve terminals, ~1 cm of the muscle nerve was freed of connective tissue and placed in a hook-in-oil electrode (Lichtman and Wilkinson, 1987). Stimulation was by negative rectangular pulses of 200 μsec duration and 2–10 V amplitude. In some experiments, the bath was made low in Ca^{2+} and high in Mg^{2+} (Wilkinson et al., 1992) to permit recording of subthreshold EPPs without contraction of fibers.

Anatomical methods. Scanning electron micrographs were prepared using conventional techniques. Briefly, whole-mounted preparations were fixed in 4% glutaraldehyde, dehydrated in acetone, and critical point dried. They were then sputter coated with gold and imaged.

Methods for supravital staining of snake motor nerve terminals with the mitochondrial probe 4-Di-2-ASP and the activity-dependent probe sulforhodamine 101 are given elsewhere (Lichtman et al., 1985; Magrassi et al., 1987; Lichtman et al., 1989). The activity-dependent probe RH-414 (Molecular Probes, Eugene, OR) was applied to the bath at 30–40 μM concentration as described by Betz et al. (1992). To incorporate activity-dependent probes the muscle nerve was stimulated supramaximally at 50 Hz for 5–10 min and the preparation immediately rinsed. Stained living preparations were imaged with a water-immersion objective on an upright microscope equipped with fluorescence optics. Images were recorded with an SIT (silicon intensified target) camera attached to an image processor (151, Imaging Technology, Woburn, MA) and video printer (Sony UP-5000). The method for acetylcholinesterase staining is described by Lichtman and Wilkinson (1987).

Results

Isolated nerve terminals

Snake neuromuscular terminals comprise ~20–60 discrete boutons arranged as a compact plate-like ending (Wilkinson and Lichtman, 1985; Lichtman et al., 1989). Two morphological changes occurred when terminals were isolated using our method. First, the terminal as a whole became smaller (and apparently thicker) and no longer corresponded in size to its former endplate site (Fig. 1). Second, each terminal bouton appeared to become nearly spherical (ellipsoidal), regardless of its former (usually irregular and relatively flat) shape when in contact with the endplate (Fig. 1; see also Fig. 6*C*). Both changes were evident in scanning electron micrographs (SEMs) of isolated terminals, as shown in Figure 2. The SEMs also suggested that shrinkage of terminals was due to elasticity of the dense connective tissue present in the muscle. Evidently, the connective tissue strands overlying a terminal were severed when the terminal was tugged from its endplate, such that segments of the strands remained with the terminal. If the strands were under slight tension *in situ,* their severed portions might contract, moving the isolated boutons closer together by forming a three-dimensional structure in lieu of the near-planar structure of the terminal while in contact with the endplate site. The same connective tissue was presumably responsible for the spontaneous movement of most terminals away from their endplates once they were freed. The distance separating the detached terminal and its former endplate site in Figure 1 is typical. Also (although not in this example) the terminal usually moved a few micrometers vertically, either upward above the plane of the endplate site or downward (and laterally) into the space separating adjacent fibers. We have no evidence to explain the change in shape of individual boutons when they were removed from the endplate. Perhaps adhesion molecules constrain them to the shape of the postsynaptic surface even though their minimum surface energy corresponds to a near-spherical shape. We have not yet studied the fate of cellular components of the muscle associated with NMJs (e.g., Schwann cells) upon terminal removal, or that of the extracellular matrix.

Viability of terminals subjected to various isolation protocols was assessed by two criteria: ability to take up supravital mitochondrial probes such as 4-Di-2-ASP (Margrassi et al., 1987; Herrera and Banner, 1990), which label only healthy terminals in a variety of species, and ability to take up activity-dependent probes in a stimulus-dependent manner (Lichtman et al., 1985; Betz et al., 1992). Neither criterion was met by isolated terminals that underwent enzyme exposures longer than those described in Materials and Methods, for example, terminals that became detached from their endplate site solely by means of enzyme treatment. In these cases mitochondrial probes did not label the

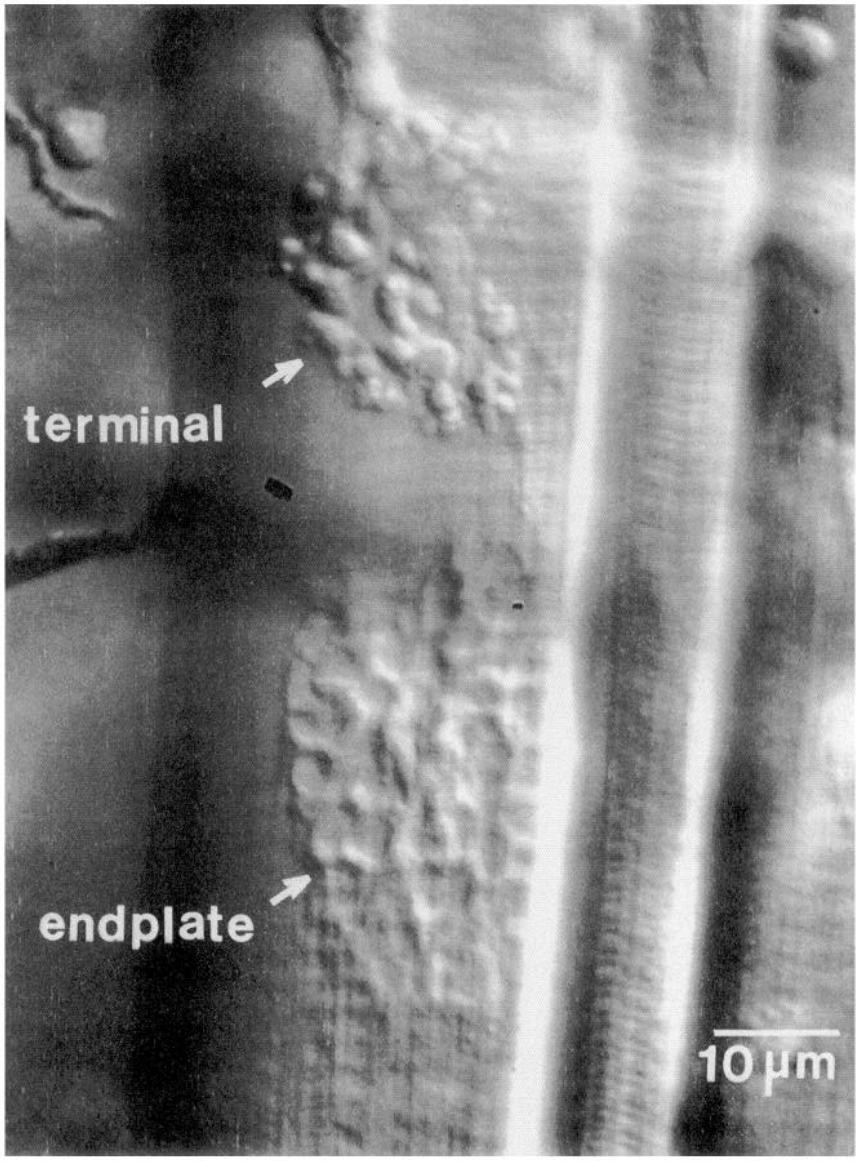

Figure 1. Living neuromuscular junction (NMJ) in the single-fiber-thick snake transversus abdominis muscle. The nerve terminal has been detached from its former endplate site using the procedure described in Materials and Methods. Outlines of various shapes on the endplate site correspond to previous locations of terminal boutons. The detached boutons are nearly spherical, unlike their previous shapes revealed by the outlines. The boutons have also drawn together such that the terminal is smaller than the endplate site. Nomarski videomicrograph.

Figure 2. Scanning electron micrograph of a detached nerve terminal similar to that shown in Figure 1. Note that some connective tissue strands remain attached to the terminal, and that the boutons (*arrows*) have assumed a near-spherical shape.

terminal boutons while activity-dependent probes were taken up without stimulation. Both observations were consistent with cell damage or death, that is, absence of mitochondrial membrane voltage gradients, disruption of the plasma membrane to allow entry of activity-dependent probes without vesicle recycling, or conditions (e.g., depolarization) that permit entry of probes as a result of continuous vesicle recycling. In contrast, terminals subjected to minimal enzyme treatment followed by mechanical dissociation took up mitochondrial probes (12 experiments; Fig. 3), and did not take up activity-dependent probes unless they were stimulated (six experiments; Fig. 4) or depolarized with KCl (eight experiments; data not shown). Focusing up and down revealed that all boutons of such terminals took up the probes. Indeed, boutons of isolated terminals were often stained more brightly than those of control terminals. One explanation for the increased brightness is the greater thickness (and hence longer optical path length) of isolated boutons upon assumption of a near-spherical shape. Our general conclusion from experiments with mitochondrial and activity-dependent probes was that terminals could survive substantial mechanical

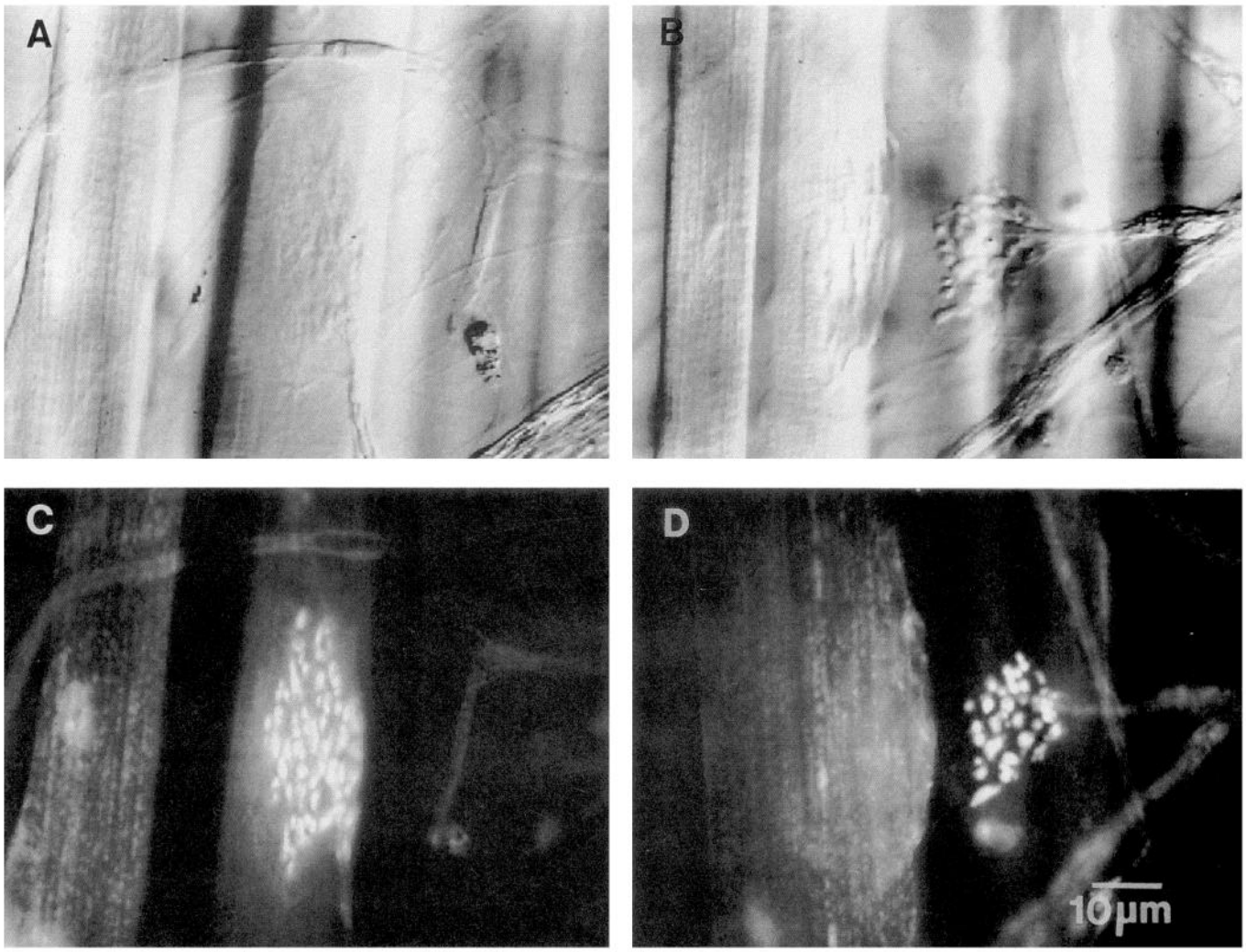

Figure 3. Uptake of the supravital mitochondrial probe 4-Di-2-ASP by snake nerve terminals. Shown in *A* is a living intact NMJ (type F fiber), and in *B* a terminal (*right*) that was detached from its former endplate site (*left*; type S fiber) in same preparation as *A*. Addition of the probe to the bath (10 μM) after terminal detachment resulted in staining (*C*) of the control terminal and (*D*) of the detached terminal, indicating that both were healthy. Punctate staining of muscle fibers in *C* and *D* is due to an abundance of large mitochondria in type S fibers. *A* and *B*, Nomarski videomicrographs; *C* and D,, videomicrographs with fluorescein epifluorescence optics.

tugging but not excessive treatment with proteolytic enzymes. Indeed, terminals that were removed after deliberately insufficient enzyme treatment (see Materials and Methods) took up both probes appropriately even though some of their interbouton connectives were severed.

Vacant endplate sites

Vacant snake endplate sites have long been used for study of presumably normal ACh receptor function (e.g., Kuffler and Yoshikami, 1975; Dionne and Liebowitz, 1982). We saw no indication of damage to muscle fibers or their endplate sites by enzymes unless treatment proceeded beyond the point of spontaneous terminal detachment, similar to the observations of Betz and Sakmann (1973) on the frog NMJ. In contrast, material in the synaptic cleft, including AChE, is destroyed or removed by collagenase or protease treatment of frog NMJs (Hall and Kelly, 1971; Betz and Sakmann, 1973; Nystrom and Ko, 1988). We also found no AChE activity when treatment proceeded to the point of spontaneous terminal detachment (three experiments). However, our usual protocol resulted in only partial removal of AChE, as inferred from histochemical staining for AChE activity (four experiments; Fig. 5).

Synaptic reconstruction

After detachment of terminals, the vacant endplate site was viewed on a video monitor at high overall magnification (~10,000) to confirm that no boutons remained attached to the endplate. The fiber was then impaled and recorded from for several minutes to confirm the absence of MEPPs that are produced by such boutons (Wilkinson and Lunin, 1992). Any postsynaptic site having visible attached boutons or MEPPs was rejected from the study, as was the corresponding terminal. Most reconstructed NMJs studied were formed by recombining a terminal with its own original endplate site (Fig. 6). This was done in either of two ways. In the first ("poor fit"; Fig. 6*C*), the terminal was deliberately misaligned with the endplate so that only approximately one-half of its boutons were potentially in contact with receptors. In the second ("good fit"; Fig. 6*D*), the terminal was manipulated into registration with the endplate as precisely as possible. With either configuration, MEPPs and

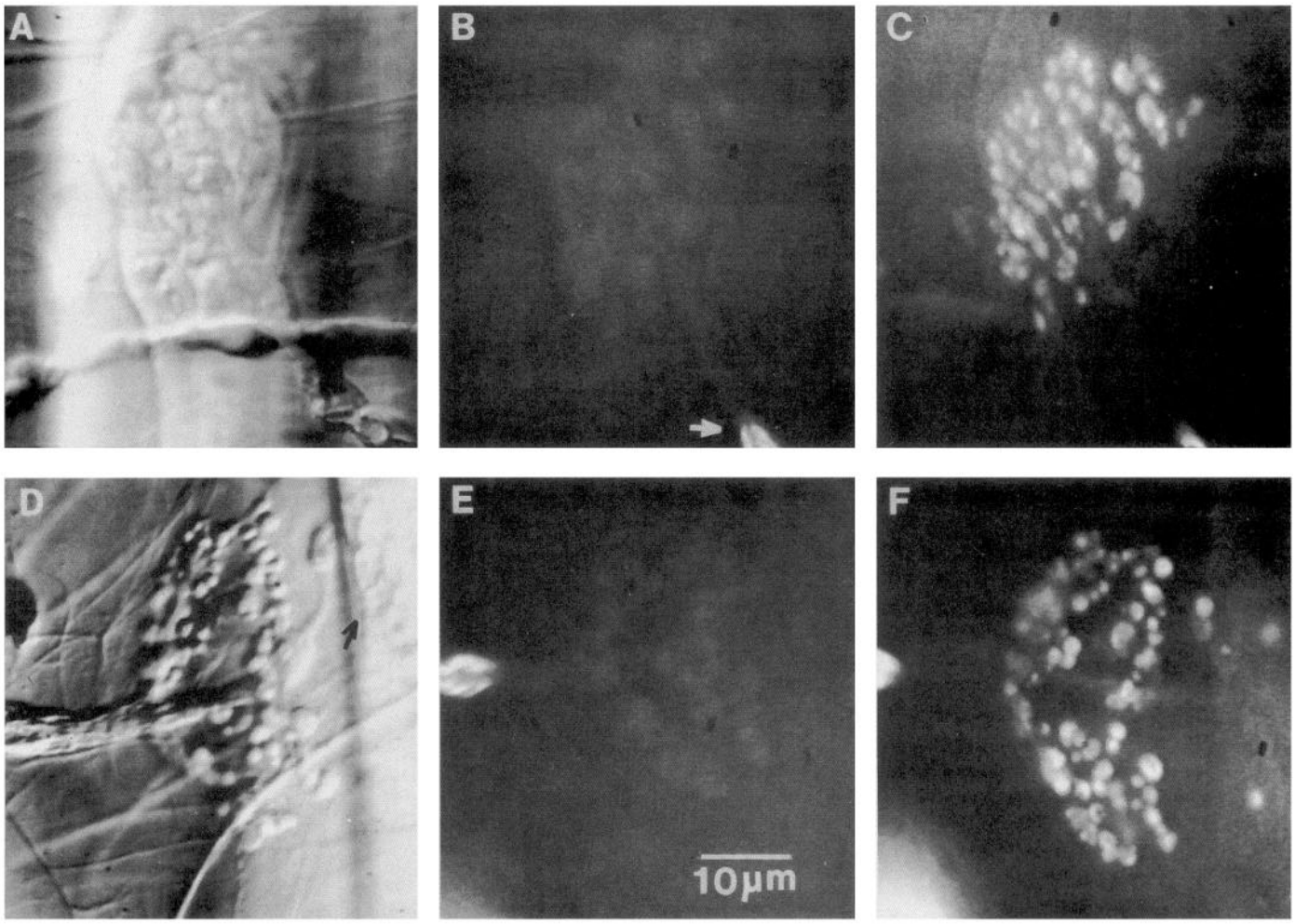

Figure 4. Activity-dependent uptake of the fluorescent probe RH-414 by snake nerve terminals. *A–C* show a typical intact NMJ in a control muscle; *D–F* show a detached nerve terminal in a different muscle. Both muscles were subsequently subjected to the identical staining procedure. *A,* Intact NMJ. *B,* Light background staining of inactive nerve terminal 20 min after addition of RH-414 (30 μM) to the bath. The probe is taken up by myelin; note last myelinated node of the terminal's axon branch (*arrow*). *C,* Stimulation (50 Hz, 5 min) of the muscle nerve labeled the terminal, presumably due to release of transmitter and recycling of vesicles. *D,* Detached nerve terminal; former endplate site at *upper right* (*arrow*). *E,* Background staining of detached terminal. *F,* Stimulation of the muscle nerve caused the terminal to take up the probe in the same manner as the terminal of an intact NMJ; focusing up and down revealed that all boutons were labeled. Results were identical using the activity-dependent probe sulforhodamine 101, or when bath-applied KCl (60 mM) was used to depolarize the terminal in lieu of nerve stimulation. *A* and *D,* Nomarski videomicrographs; *B, C, E,* and *F,* videomicrographs with rhodamine epifluorescence optics.

evoked endplate potentials (EPPs) could be recorded immediately (~200 msec or less) upon contact between terminal and endplate (see below). Reconstruction of NMJs from a terminal and a foreign endplate site ("mixed" NMJs; see below) was performed exclusively in the "good fit" configuration. In the experiments described below, control records refer to those obtained from intact NMJs in normal reptilian saline before treatment with enzymes. Additional control records obtained in some experiments after collagenase treatment alone, or after collagenase plus protease treatment but without terminal detachment, were similar (data not shown) excepting that protease treatment appeared to hyperpolarize and increase the membrane time constant of some muscle fibers (see below).

Spontaneous synaptic events

A typical MEPP recorded from a reconstructed NMJ is shown in Figure 7. Also shown are a control MEPP recorded from the same NMJ before the preparation was subjected to enzyme treatment, and a typical MEPP from an intact NMJ in a bath containing the anticholinesterase agent neostigmine at near-maximal blocking concentration (1 μM; dose response determined in separate experiments). The records are manually aligned on the time axis to illustrate that both rise times and fall times were slightly lengthened by the reconstruction process. To quantitate change in time course of MEPPs, events were recorded from each class of NMJ described above and fit individually to single exponentials to estimate their rising (τ_r) and falling (τ_f) time constants. These were (τ_r, mean ± SD, N = 5 NMJs of each class, six events/NMJ) 0.82 ± 0.30 msec (control), 0.97 ± 0.38 msec (reconstructed), 1.1 ± 0.55 msec (neostigmine), and (τ_f, mean ± SD, N = 5 NMJs of each class, six events/NMJ) 4.4 ± 2.0 msec (control), 5.3 ± 2.6 msec (reconstructed), 9.5 ± 4.0 msec (neostigmine), respectively. Thus, average MEPP rise times and fall times at reconstructed NMJs were lengthened ~20%, and the range of rise and fall times (SDs) increased ~30%, that is, slightly more than proportionately. The change

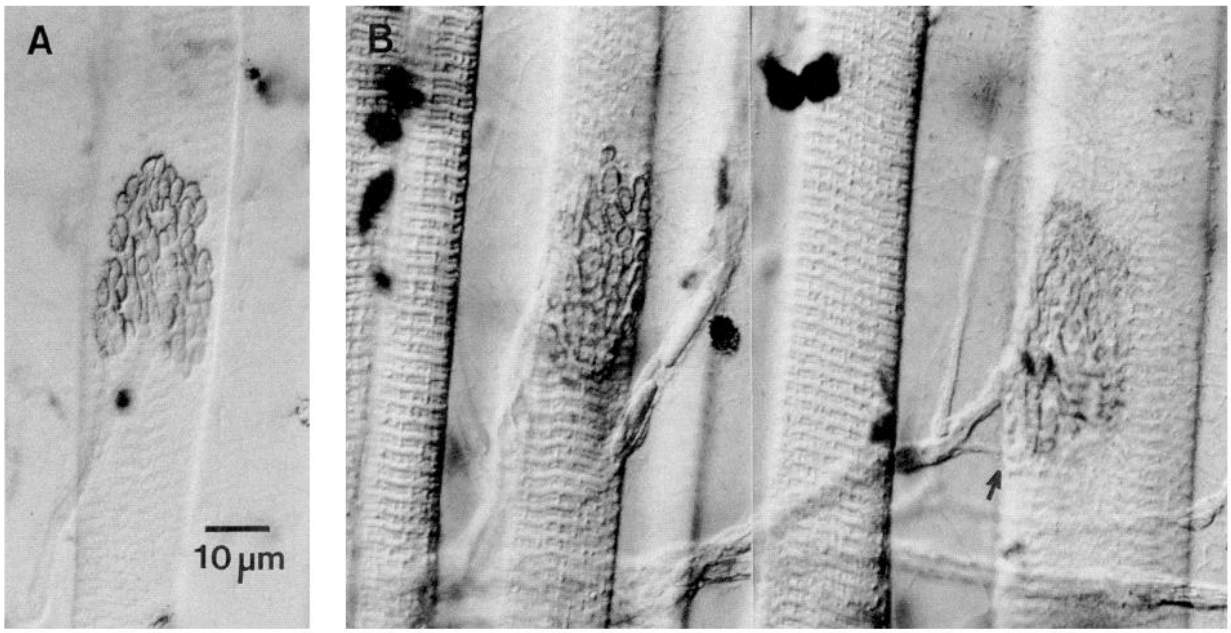

Figure 5. AChE activity at snake twitch fiber endplate sites (Nomarski photomicrographs). *A,* Typical AChE staining of an intact NMJ in an untreated control preparation. *B,* AChE staining of two neighboring endplates in an enzyme-treated preparation (same AChE staining procedure as in *A*). At *left* is an intact NMJ. Staining is similar to the untreated NMJ in *A,* indicating that collagenase pretreatment had little effect on AChE. Note that staining underneath each terminal bouton is lighter than that within a thin outline surrounding the bouton, perhaps because accessibility of staining reagents was reduced by the narrow synaptic cleft. At *right* is an endplate site (type S fiber) whose terminal (*arrow*) was detached (all but a few boutons are out of focus *below* and *left* of the fiber). Staining intensity suggests that a substantial fraction of the AChE remained. The staining pattern reflects the former location of boutons and is nearly uniform, presumably due to accessibility of the entire postsynaptic membrane to staining reagents.

in MEPP time course seen after reconstruction therefore resembled that produced by neostigmine, but was less severe.

Anticholinesterases increase MEPP amplitudes as well as rise times, due to increased amplitude and duration of the underlying MEPCs. In contrast, the reconstruction process did not significantly alter mean amplitude of MEPPs. This is shown in Figure 8, which presents amplitude histograms of MEPPs recorded from the same NMJ under three conditions: before any enzyme treatment (control), after the terminal was detached and the NMJ reconstructed with the best obtainable alignment between terminal and endplate ("good fit"), and after the terminal was moved laterally on the surface of the muscle fiber so that only approximately one-half of its boutons were in contact with the endplate ("poor fit"). Although mean MEPP amplitudes were unchanged, the distribution of MEPP amplitudes about the mean widened considerably upon reconstruction (Fig. 8). This was seen at all reconstructed NMJs examined for which control MEPP histograms were obtained ($N = 7$).

Also changed were MEPP intervals, which increased (frequency decreased) upon reconstruction for six NMJs (example in Fig. 9) and decreased slightly for one. The factor by which the mean interval increased varied considerably among preparations (3.5 ± 3.0; mean $\pm$ SD), suggesting that more than one determinant of spontaneous release rate may have been modified by reconstruction (see Discussion). Exposure to collagenase treatment alone had no effect on MEPP intervals. We also compared MEPP intervals at the same NMJ reconstructed with differing overlap between terminal and endplate. In each of three experiments, the mean MEPP interval increased monotonically as the number of terminal boutons in contact with the endplate decreased. The reconstructed NMJ of Figures 8 and 9, for example, exhibited a mean MEPP interval of 1.3 sec with maximum overlap (good fit). The mean interval increased by a factor of 3 when the terminal was displaced so that only about one-half of its boutons contacted the endplate (Fig. 9).

MEPPs (and EPPs, described below) were "all or none" in the sense that we were unable to grade their amplitude or rise time by varying the distance between terminal and endplate, a procedure expected to affect transmitter diffusion. To examine this unexpected property of reconstructed NMJs, a terminal was manipulated directly above (but not contacting) the endplate region of a twitch fiber, and the fiber was impaled. The terminal was carefully manipulated downward into contact with the endplate, at which time MEPPs appeared. Raising the terminal ~ 0.5 μm above the endplate (according to the calibrated dial of our micromanipulator) caused an immediate cessation of MEPP activity (or its disappearance into the noise, which was <50 μV peak–peak at 1 kHz bandwidth). Relowering the terminal an approximately equal amount caused MEPPs to reappear, again in an "all or none" manner. MEPPs could be gated on and off repeatedly by this technique of slightly raising and lowering the terminal (Fig. 10). In no case were MEPPs of intermediate character observed (i.e., slower rise time, or decreased but still measurable amplitude). Invariance of MEPP amplitudes in this regard was examined and confirmed by recording 100 events, then raising a terminal, then lowering the terminal and recording 100 events, and so on, for a total of three or four trials. Mean MEPP amplitudes varied $<9\%$ among four trials in each of three such experiments and $<15\%$ among three trials in the fourth experiment.

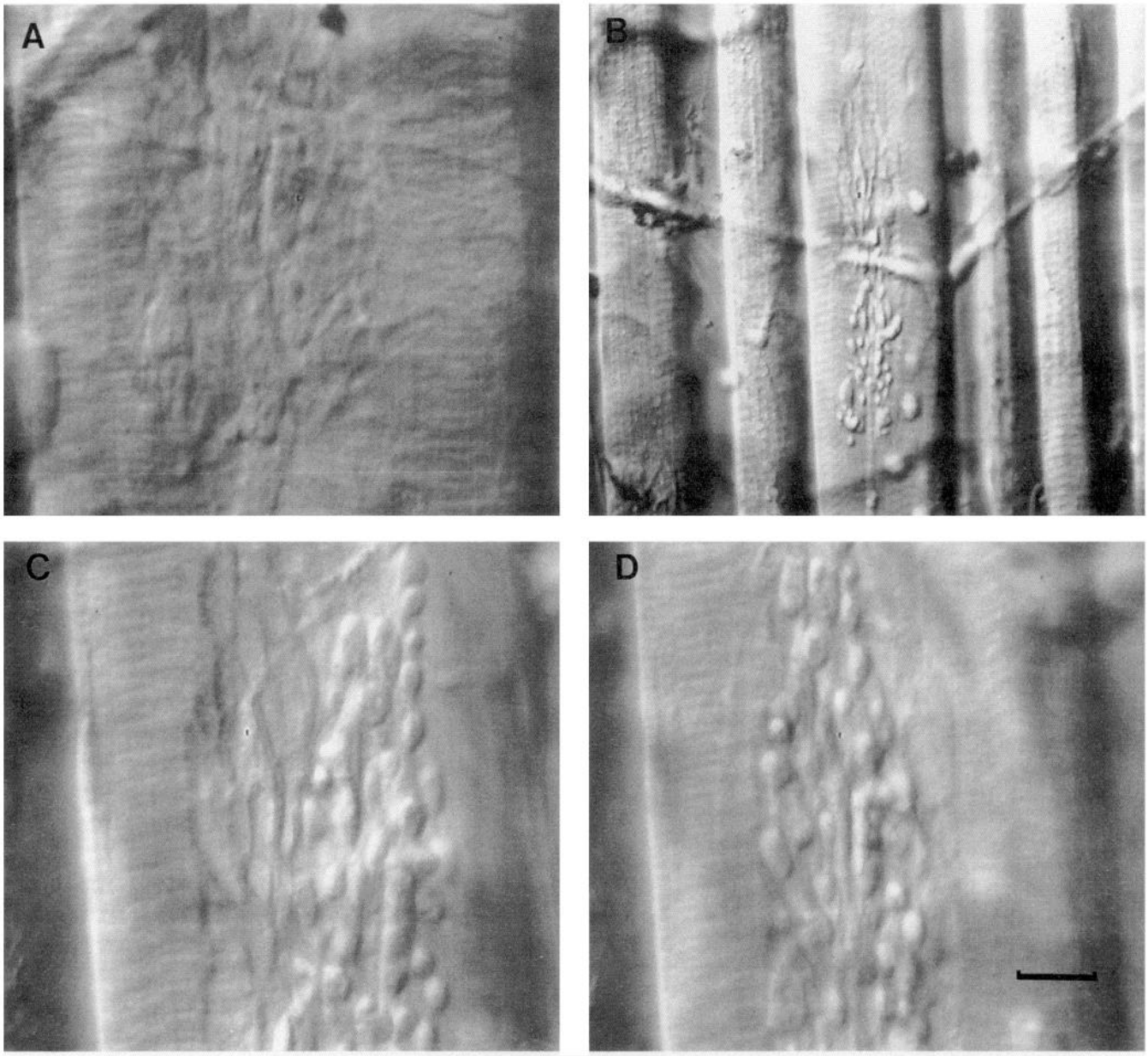

Figure 6. Technique used for reconstruction of snake NMJs. *A,* An NMJ was visualized and selected for study. *B,* During or just after local application of protease and Ca^{2+}, the terminal was gently tugged away from its endplate site (in the photo's downward direction) by manipulating connective tissue with a glass pipette (out of focus; note sharp bend in lymphatic vessel evidently attached to the same connective tissue). *C,* After rinsing, the terminal was manipulated with a similar pipette and positioned so that approximately one-half of its boutons were in contact with the endplate site ("poor fit"). *D,* Alternatively, the terminal was positioned to obtain the best possible registration between terminal and endplate site ("good fit"). Nomarski videomicrographs. Scale bar: 6 μm for *A, C,* and *D*; 20 μm for *B.*

Evoked responses

Endplate potentials (EPPs) were recorded in response to supramaximal stimulation of the muscle nerve with bath Ca^{2+} and Mg^{2+} adjusted to prevent muscle contraction (see Materials and Methods). EPPs at reconstructed NMJs exhibited lengthening of rise and fall times, similar to spontaneous MEPPs (Fig. 11*A*; compare to Fig. 7). Lengthening of rise times was 23% ± 10% (mean ± SD, $N = 5$ NMJs, six events/NMJ), approximately the same factor found for MEPPs. Unlike MEPPs, however, amplitudes of EPPs were reduced by reconstruction and depended on the number of boutons placed in contact with the endplate. Shown in Figure 12 are sequential oscilloscope traces of EPPs recorded from a typical NMJ (fast twitch) before enzyme treatment (control), and after reconstruction with best alignment of terminal and endplate ("good fit"). EPPs were recorded in these configurations and also after the terminal was shifted so that approximately one-half of its boutons were no longer in contact with the endplate ("poor fit"). MEPPs were recorded in each configuration. Mean quantal content was 20 for the native NMJ, 11 after reconstruction with "good fit," and 7 after reconstruction with "poor fit." Because MEPP amplitudes did not change significantly with reconstruction (see Fig. 12 legend), these relative quantal contents reflect similar ratios in EPP amplitudes (45% of control amplitude after reconstruction with "good fit"). In three additional experiments, mean

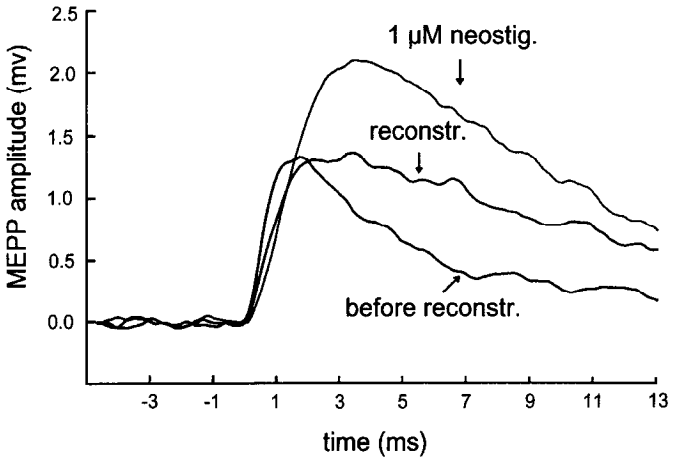

Figure 7. Example of spontaneous potentials (MEPPs) from two NMJs in the snake transversus abdominis muscle. Shown are digitized records from a typical twitch fiber NMJ (*before reconstr.*), and from the same NMJ after terminal dissociation and reconstruction (*reconstr.*). The rising phase and (usually) the passive decay of MEPPs were prolonged by the reconstruction process. Also shown is a typical MEPP from an unreconstructed NMJ recorded with the anticholinesterase agent neostigmine added to the bath (*1 μM neostig.*). Lengthening of the MEPP rising phase due to reconstruction was less than that due to AChE blockade. Relative amplitudes of the three classes of MEPPs are typical; see Figure 8.

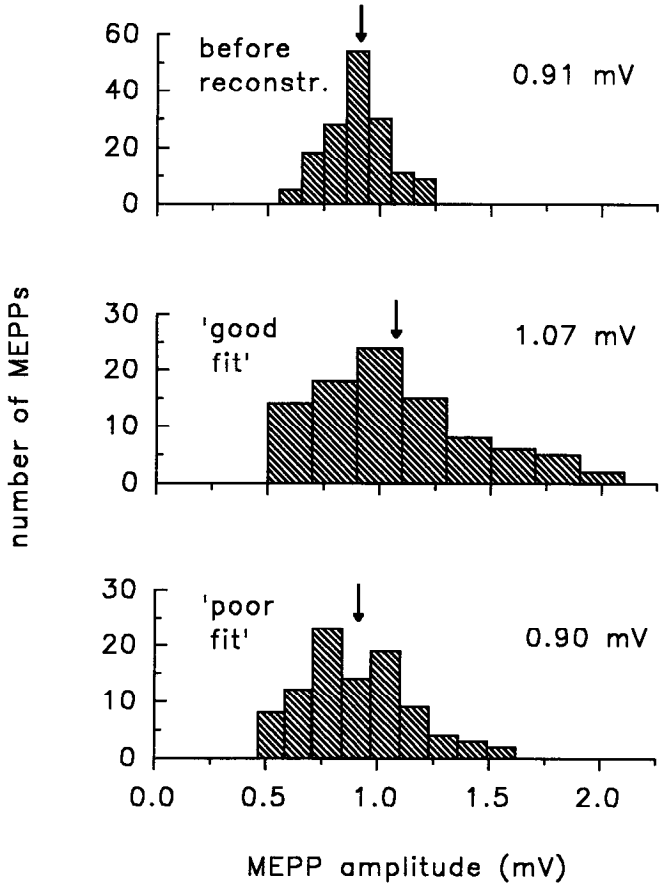

Figure 8. Amplitude histograms of MEPPs recorded from one NMJ (type S fiber). *Arrows* point to numerical means of distributions, shown at *upper right*. Initially (*before reconstr.*) MEPPs had a mean amplitude of 0.91 mV (mean corresponding to peak of best Gaussian fit, 0.85 mV). Reconstruction of the NMJ with optimum alignment between terminal and endplate site (*'good fit'*) did not significantly alter the mean MEPP amplitude (1.07 mV; Gaussian peak, 0.86 mV), nor did reconstruction with deliberate misalignment between terminal and endplate site (*'poor fit'*; about one-half of the terminal boutons did not contact the endplate site; mean, 0.90 mV; Gaussian peak, 0.89 mV). Amplitude histograms were consistently broadened by either type of reconstruction.

EPP amplitude was 40% ± 20% (average ± SD) of control amplitude upon reconstruction (all "good fit"). In a fourth experiment, mean EPP amplitude decreased only slightly (from 7.2 mV to 6.4 mV). EPPs at reconstructed NMJs underwent quantal fluctuations without failures in low Ca^{2+} bath solution, similar to controls (Fig. 12). In three of four preparations tested, restoration of normal Ca^{2+} to the bath resulted in superthreshold EPPs, muscle fiber action potentials, and contractile activation (Fig. 11*B*). In contrast to the situation when recording MEPPs, slight lifting of the terminal above the endplate (~0.5 μm) did not completely abolish measurable EPPs. Their amplitude diminished substantially, however, and occasional failures occurred (Fig. 13). Rise times of EPPs from slightly lifted terminals were not altered (data not shown; see Discussion).

"Mixed" NMJs

Functional synapses were also formed by combining vacant endplate sites with foreign terminals detached from nearby endplates. These mixed NMJs exhibited the same general behavior (described above) as did NMJs reconstructed from terminals and their original postsynaptic partners. We utilized mixed NMJs to examine the regulation of quantal size in snake muscle. It is known that large, high-input-conductance (high G_{in}) muscle fibers receive larger single quantal currents (miniature endplate currents, MEPCs) than do small, low G_{in} fibers in the same muscle (Wilkinson et al., 1992). However, it is not clear whether this apparent regulation of single quantal current according to target requirements occurs presynaptically (e.g., larger transmitter vesicles for high G_{in} fibers) or postsynaptically (e.g., higher receptor density for high G_{in} fibers). To address this question we selected pairs of NMJs in one muscle that differed substantially in G_{in} (usually a small S fiber and a large F fiber) and reconstructed NMJs having all four possible terminal-on-endplate site configurations (S terminal on S endplate site, S terminal on F endplate site, F on F, F on S). MEPPs were recorded for each configuration, and MEPC amplitudes calculated as MEPP amplitudes × G_{in} (see Materials and Methods). MEPC histograms, mean MEPC amplitudes, and example records from one experiment are presented in Figure 14. MEPCs were smaller for reconstructed NMJs containing the S endplate site (1.2 nA; average of S on S and F on S) and larger for reconstructed NMJs containing the F endplate site (1.6 nA; average of S on F and F on F). In this particular experiment, a third isolated terminal (T) from a small tonic fiber with very low G_{in} was within reach of the S endplate site. The T on S reconstructed NMJ produced MEPCs similar in amplitude to the S on S and F on S combinations (Fig. 14). Results were the same in two additional experiments. In the first, the synaptic components of a small S fiber (G_{in}, 0.714 μS) and a large F fiber (G_{in}, 1.20 μS) were reconstructed in all four combinations. Mean MEPC amplitudes (71–121 events recorded in each configuration) were 0.43 nA (S on S) and 0.49 nA (F on S) when the smaller fiber's endplate was the target, both smaller than 0.68 nA (F on F) and 0.65 nA (S on F) when the larger fiber's endplate was the target. In the second experiment, G_{in} of the small S fiber was 0.625 μS while

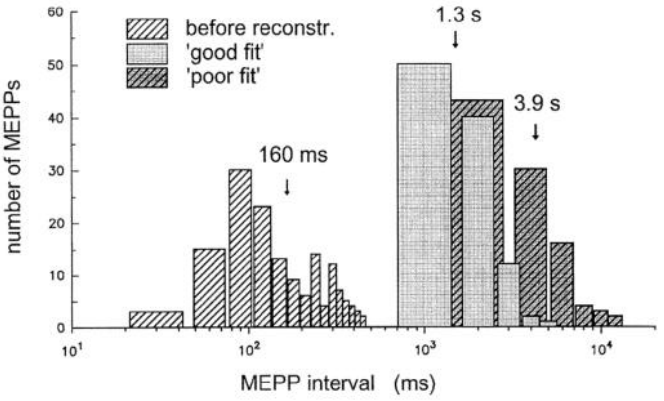

Figure 9. Interval histograms for records whose MEPP amplitude histograms are shown in Figure 8 (logarithmic time axis). Mean intervals for each class are depicted by *arrows*. MEPPs occurred less frequently after synaptic reconstruction, although the factor by which their mean interval increased varied widely among preparations (see Results). MEPP intervals at reconstructed NMJs depended inversely on the number of boutons in contact with the endplate site. In this example, removal of about one-half of the boutons from the endplate site of a reconstructed NMJ increased the mean MEPP interval from 1.3 sec to 3.9 sec.

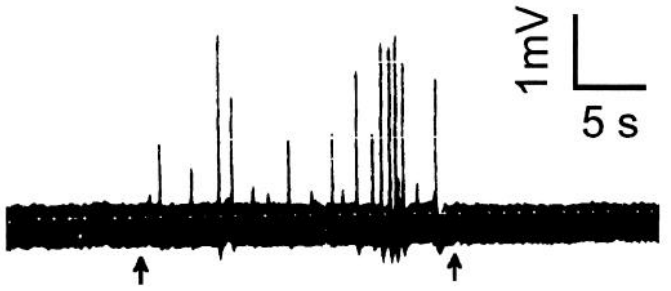

Figure 10. Photograph of a single storage oscilloscope trace (1–3 kHz bandwidth) illustrating the "all or none" character of MEPPs at a reconstructed NMJ. Just before the trace began, a detached terminal was manipulated over its former endplate site and lowered until MEPPs appeared in the intracellular record. The terminal was raised ~0.5 μm, and MEPP activity promptly ceased. The terminal was lowered ~0.5 μm (*left arrow*), which resulted in resumption of MEPP activity. The terminal was again raised ~0.5 μm (*right arrow*) and MEPP activity again ceased. Baseline noise is low frequency and due in part to slow storage oscilloscope sweep speed. Resting potential, −97 mV.

G_{in} of the large F fiber was 0.893 μS. Mean MEPC amplitudes (average of two trials per configuration, 28–58 events/trial) were again smaller when the S endplate was the target, namely, 0.69 nA (S on S) and 0.63 nA (F on S) compared to 1.11 nA (F on F) and 1.23 nA (S on F). Thus, in all cases the mean MEPC amplitude was apparently determined by G_{in} or some related attribute of the postsynaptic cell (small or large; S or F), and not by the presynaptic terminal.

Discussion

Snake NMJs contain discrete presynaptic boutons, similar to mammalian CNS and autonomic synapses. Each bouton comprises approximately seven active zones that collectively release one to three transmitter quanta when activated at low stimulus frequencies (Wilkinson, 1988). Thus, like boutons at vertebrate central synapses (e.g., Korn et al., 1982), each snake neuromuscular bouton is the anatomical substrate for release of about one quantum. The experiments described are most easily interpreted at the level of single boutons. As argued below, they are consistent with the hypotheses that (1) synapses of individual boutons within reconstructed NMJs either function nearly normally or do not function at all, and (2) close contact between a bouton and some region of the endplate site is necessary for function.

Spontaneous events

MEPP frequency diminished substantially after reconstruction, suggesting that only a fraction of boutons (or active zones) were capable of synaptic function, even in the good fit configuration. The number of nonfunctional boutons (or active zones) was about one-half of those placed over the endplate, based on MEPP frequency. This is only a rough average, as some boutons of a particular terminal might have undergone an increase in rate of spontaneous release as a result of enzymatic and mechanical manipulation, while the observable release rate of others may have decreased. Remarkably, all MEPPS observed at reconstructed NMJs had nearly normal characteristics (see below), and their frequency was proportional to the number of boutons held in firm contact with the endplate ("good fit" vs "poor fit").

Three abnormalities of MEPPs were observed when behavior of reconstructed NMJs was compared to control NMJs: longer rise times, longer fall times (in most experiments), and a broadening of MEPP amplitude histograms (although mean MEPP amplitudes were not significantly affected). Because the MEPP rising phase corresponds to the duration of the MEPC, its lengthening is consistent with prolongation of transmitter binding and/or a broader range of diffusion times among ACh molecules at one endplate. The latter influence was expected due to the likelihood that pre- to postsynaptic alignment was unfavorably altered, but we were surprised that the increase in rise times was small and relatively uniform. Indeed, the range of rise times observed was only slightly greater than that of controls, and we failed to detect any events with particularly long rise times. AChE activity was somewhat diminished by protease treatment (judged roughly by histochemical staining intensity), which may also have contributed to slowing of rise times in a manner similar to action of the drug neostigmine (Katz and Miledi, 1973). Lengthening of the MEPP falling phase usually occurred, possibly reflecting change in postsynaptic passive membrane properties (e.g., resistance increase), which were not studied. Consistent with this possibility, we noted a slight (although not statistically significant) hyperpolarization of muscle fiber resting potentials after enzymatic treatment for about one-half of the reconstructed NMJs examined. The observed consistent broadening of MEPP amplitude histograms without concomitant change in mean MEPP amplitude indicates that some MEPPs diminished in amplitude while others increased. One explanation is that partial removal of AChE (and possible increase in postsynaptic membrane resistance) tended to increase MEPP amplitudes, while at the same time other consequences of reconstruction (e.g., longer transmitter diffusion distances) tended to diminish amplitudes. A second explanation for increase in amplitude of some MEPPs is possible narrowing of the synaptic cleft in some regions after enzymatic removal of material. Additional experiments employing direct intracellular and extracellular measurement of MEPCs, and under controlled conditions of AChE blockade, are needed to address these unresolved questions.

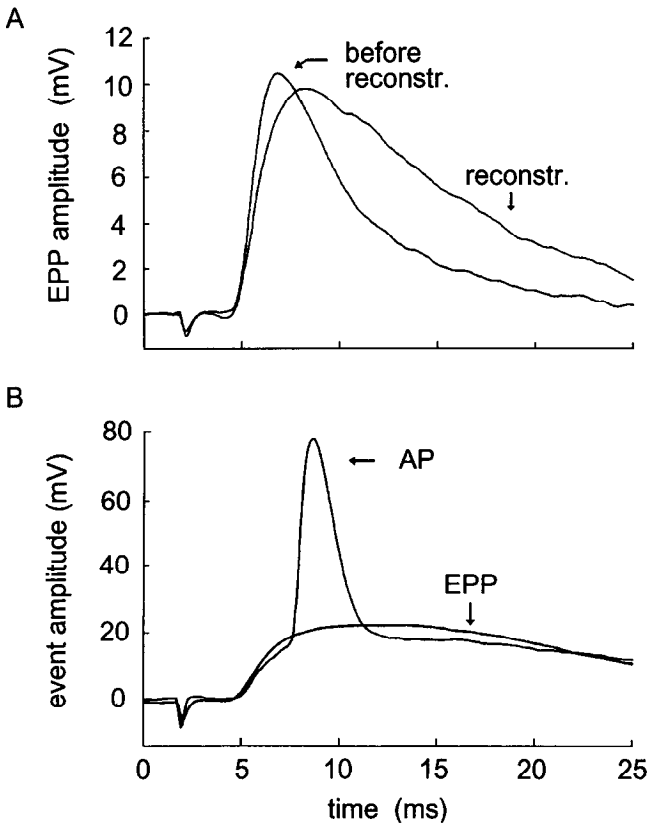

Figure 11. Example of evoked endplate potentials (*EPP*) from one snake NMJ. The muscle nerve was supramaximally stimulated (negative-going artifact at *left*) and EPPs were made subthreshold by adjusting levels of Ca^{2+} and Mg^{2+} in the perfused bath. *A*, A twitch fiber NMJ was selected for reconstruction and control responses recorded (*before reconstr.*). The NMJ was then dissociated, perfused with the same low Ca^{2+}/high Mg^{2+} bath solution, and reconstructed. Evoked EPPs (*reconstr.*) exhibited prolonged rise and passive decay times compared to control EPPs, similar to the effect of synaptic reconstruction on MEPPs (compare Fig. 7). *B*, Perfusing the bath with normal reptilian saline caused responses to rise rapidly in amplitude (*EPP*) until they became superthreshold (*AP*). Records are uncorrected for resting potential (−78 mV before, −72 mV after reconstruction).

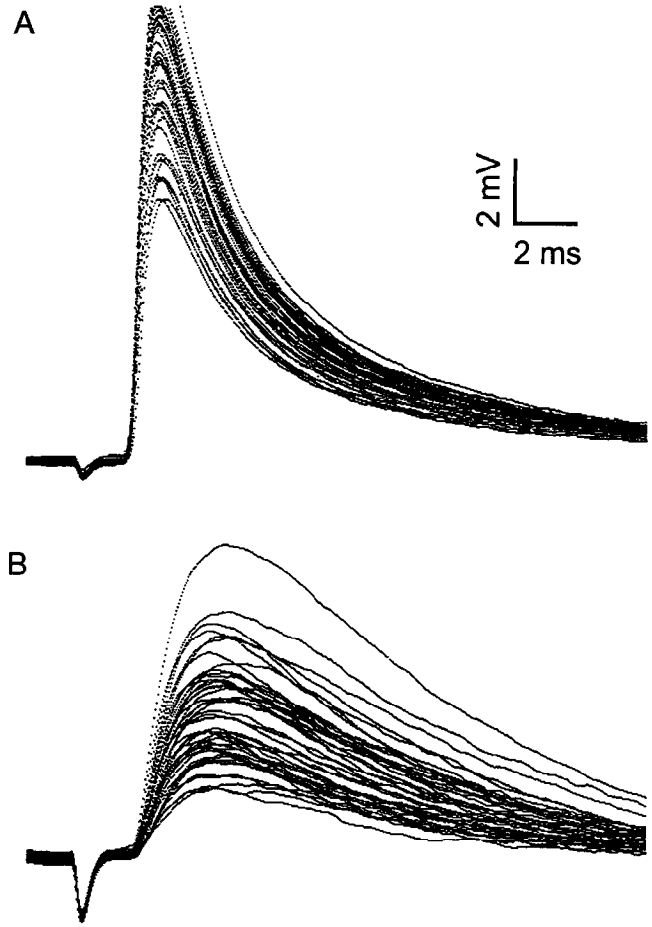

Figure 12. Quantal fluctuations among evoked subthreshold EPPs at an NMJ before (*A*) and after (*B*) reconstruction. Each series shows responses to 46 sequential stimuli (0.25 Hz frequency; negative artifact at *left*) delivered to the muscle nerve with the same low Ca^{2+}/high Mg^{2+} bath perfusate; no records are omitted. Note absence of failures, and quantal fluctuations of approximately the mean MEPP amplitude (0.65 mV before, 0.70 mV after reconstruction). Records shown are uncorrected for resting potential (−85 mV in *A*, −88 mV in *B*) and nonlinear summation. Mean quantal content after corrections was 20 in *A* and 11 in *B*.

Evoked responses

Like MEPPs, EPPs recorded from reconstructed NMJs appeared nearly normal. A slowing of EPP rise times was seen; however, the rise times were no slower than those of MEPPs, consistent with a normal synchronous release process. Quantal fluctuations in low Ca^{2+} bath were present and similar to those of normal NMJs. Mean quantal content was assessed directly in some preparations and was on average about one-half of normal for a particular bathing solution composition. Furthermore, mean quantal content was proportional to the degree of overlap between terminal and endplate when the two were deliberately misaligned. These observations suggest that about one-half of boutons (or active zones) formed functional synaptic contact when the terminal was optimally aligned, the same fraction as that deduced from study of MEPPs. The necessity of firm contact seen during MEPP recording was also confirmed during recording of EPPs: evoked responses diminished by an order of magnitude when the terminal was raised slightly above the endplate. The remaining detectable signal fluctuated in steps of about one quantum, with occasional failures (Fig. 13). This suggests that one or a few boutons may have remained in contact with the endplate when the terminal (which is flexible) was slightly raised—supporting our contention that synaptic function of each bouton is all or none and requires firm contact with the endplate. Alternatively, several (or all) of the boutons supplying one NMJ might have remained functional, but with smaller quantal currents, when the terminal was raised. In this case, however, one would have expected smaller quantal fluctuations than we observed, with few or no failures.

Synaptic function was assayed by postsynaptic intracellular recording. Thus, the observed decreases in quantal content and MEPP frequency upon reconstruction could have resulted either from lack of functional synaptic contact or from failure of release. We consider the latter unlikely because all boutons of isolated terminals took up activity-dependent probes when stimulated. Further work is needed to study directly the effects of reconstruction on presynaptic release.

Access to synaptic components

Because of morphological evidence such as the shrinkage of detached nerve terminals and swelling of boutons, and due to

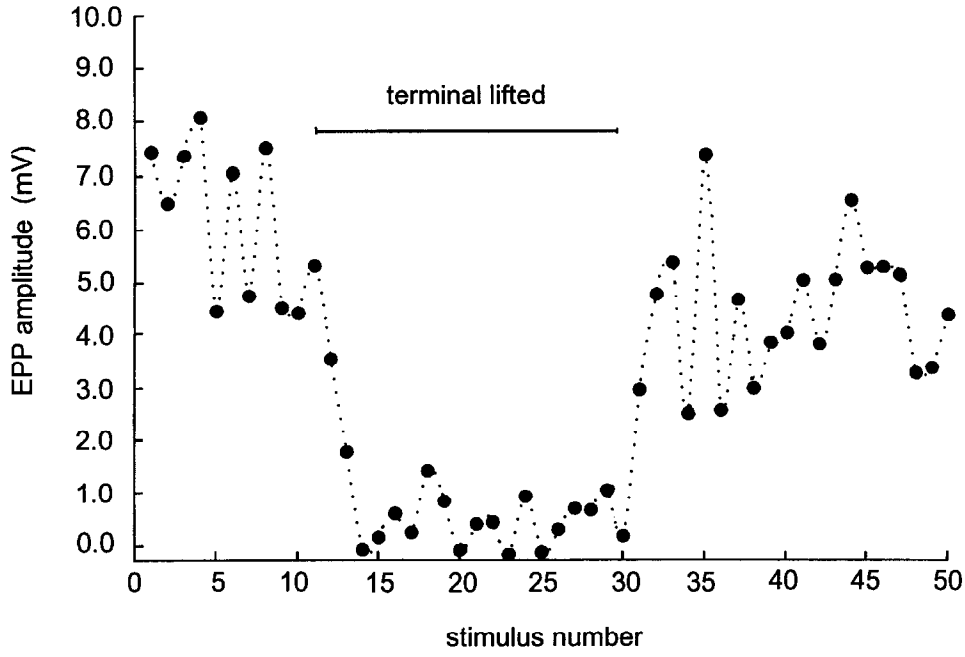

Figure 13. Peak amplitudes of subthreshold EPPs recorded from a reconstructed NMJ as in Figure 11 (resting potential, −90 mV). The muscle nerve was stimulated for 100 sec at a 0.5 Hz rate; each data point is the response to one stimulus. Raising the glass probe that held the terminal against the endplate by ~0.5 μm during stimuli 11–30 diminished EPP amplitudes by an order of magnitude but did not completely abolish EPPs. Note quantal fluctuations, and occasional failures in response to stimuli delivered while the terminal was lifted.

the limits of manual micromanipulation, it seems likely that each application of a terminal to an endplate resulted in a unique synaptic geometry. Surprisingly, MEPP rise time and amplitude statistics remained stable when an NMJ was repeatedly reconstructed, even when it was deliberately reconstructed with varying numbers of boutons in contact with the endplate site. Stability of MEPPs under these circumstances indicated not only that synaptic efficacy at the level of boutons was all or none, but also that transmitter packets from all boutons of one terminal were on average indistinguishable, and, moreover, that all regions of the endplate were on average equally sensitive. These properties of reconstructed NMJs—specifically of individual one-bouton synapses within the NMJs—were utilized as a practical tool for independent study of pre- and postsynaptic components. By combining the same terminal with the endplate sites of different fibers, differences in MEPP amplitude necessarily reflected differences in the endplate sites, and vice versa for combining the same endplate site with different terminals.

We had found previously that quantal size is positively correlated with muscle fiber input conductance. In the present study, reconstruction of mixed NMJs showed that differences in quantal size among NMJs in one muscle result from differences among the NMJs' postsynaptic components. When combined with previous studies (see introductory remarks), this finding suggests a logical symmetry of function at the NMJ: one determinant of synaptic strength, quantal content, is primarily presynaptic, while the other determinant, quantal size, is primarily postsynaptic. Just what postsynaptic structural differences exist among NMJs exhibiting different quantal size is not known. However, we emphasize that quantal size was examined in the context of relatively long-term neuron–target "matching." Quantal size also varies with activity and with certain acute experimental manipulations, via regulatory mechanisms that appear to be presynaptic (Van der Kloot, 1991).

The experimental accessibility provided by the "mixed" reconstruction technique might serve other avenues of research. In particular, synaptic processes with a memory of at least several seconds, for example, those involving second messengers or other means of slow synaptic modification, could be examined at the level of individual synaptic components. Such modifications should persist either after an intact modified synapse is dissociated, or after an isolated modified component is reconstructed into a "standard" synapse for assay of its function. For example, the structural modifications associated with potentiation, facilitation, depression, and so on, could be studied by activating an isolated terminal (or vacant endplate site) under various conditions and then assaying function of an appropriate reconstructed synapse. Another useful approach would utilize experimental manipulations that putatively reveal post- to presynaptic feedback pathways. The manipulations (e.g., application of drugs) could be performed on isolated components, or on intact synapses whose individual components are subsequently compared to controls, in order to isolate pre- and postsynaptic mechanisms.

Pre- to postsynaptic alignment

As in other vertebrates, two ultrastructural characteristics of snake twitch muscle fiber NMJs reflect precise alignment between pre- and postsynaptic components. First, the pre- and postsynaptic membranes are closely spaced, being separated by a uniform narrow cleft. Second, terminal boutons contain linear Ca^{2+} channel arrays (active zones) that are located precisely opposite postsynaptic secondary folds (e.g., electron micrographs of snake NMJs in Lichtman et al., 1989; Coniglio et al., 1993). These submicrometer-level features of intact NMJs are established in early synaptogenesis and are stably maintained in adults (Nystrom and Ko, 1988; Ko and Folsom, 1989), suggesting an important functional role. However, they were almost certainly not reestablished after synaptic reconstruction by our method. Although we found that close spacing (actual contact, within the limits of manual manipulation) was required for synaptic function, just what spacing was actually provided is unknown. Moreover, the relative positions of active zones and secondary folds were in all probability completely randomized

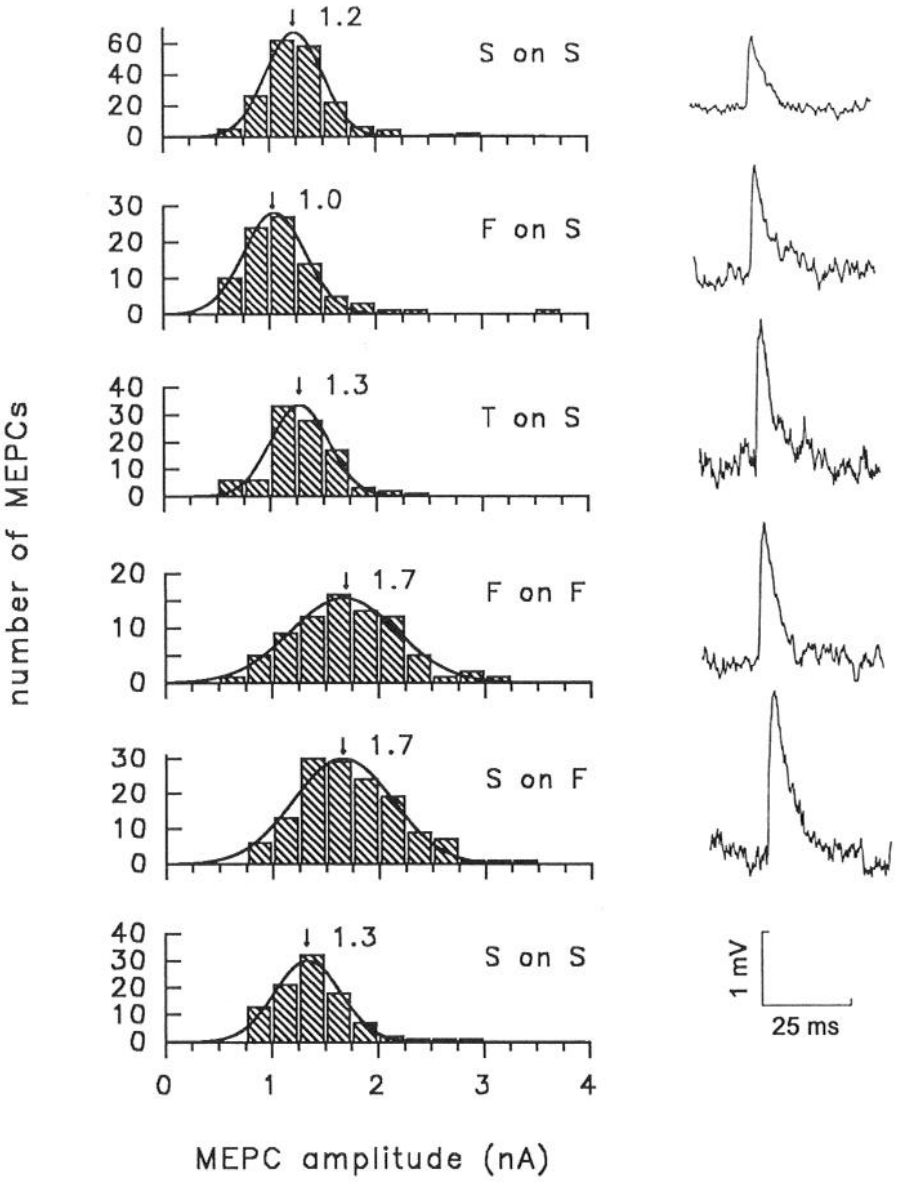

Figure 14. MEPPs at "mixed" reconstructed NMJs revealed that single quantal efficacy is mediated postsynaptically. NMJs from three fibers (small tonic, *T*, G_{in} = 0.3 μS; medium slow twitch, *S*, G_{in} = 0.8 μS; large fast twitch, *F*, G_{in} = 1.2 μS) were dissociated and reconstructed in various combinations (*F on S* means terminal formerly innervating F fiber was placed on vacant S fiber endplate site, etc.). Some combinations were not possible; for example, the T axon would not reach the F endplate. MEPPs were recorded from each combination (example records at *right*) and converted to miniature endplate currents (MEPCs; see Materials and Methods). Histograms (*left*; means indicated by *arrows* are peaks of best Gaussian fits) showed that MEPCs recorded from the F fiber were consistently larger than those recorded from the S fiber, irrespective of which presynaptic terminal supplied the innervation. Second S on S histogram (*bottom*) was recorded at end of experiment as a control. All data normalized to resting potential of −80 mV. Actual resting potentials were, for *S on S*, −92 mV; *F on S*, −92 mV; *T on S*, −90 mV; *S on F*, −91 mV; *F on F*, −90 mV. Results were the same when numerical means were used instead of Gaussian peaks.

by reconstruction. It is possible that active zone to secondary fold alignment was reestablished spontaneously after reconstruction, perhaps by movement of active zones and/or secondary folds within their respective membranes. Besides there being no evidence for such phenomena, this seems unlikely because no delay in function of reconstructed synapses after their formation was noted. However, our time resolution was only a few hundred milliseconds, and it is not clear how long such movements would require. A related possibility is that even random pre- to postsynaptic orientation results in registration of a substantial number of active zones with folds. This is perhaps plausible at the amphibian NMJ, where active zones (and folds) form a dense, nearly uniform pattern of "stripes" aligned normally to the NMJ's long axis (e.g., Betz and Bewick, 1992). However, no similar repeating pattern exists within the boutons of reptilian NMJs, where active zones are scattered and randomly oriented (Walrond and Reese, 1985). The alternative conclusion is that reconstructed NMJs totally lacked alignment between active zones and folds. If so, we saw no clear deficit in function of at least some individual active zones (i.e., in MEPPs) as a result. We emphasize that only rudimentary function at low frequencies has been assessed thus far. Function at high frequencies, or over long periods, may be impaired at reconstructed synapses, as might potentiation or other long- and short-term regulatory mechanisms.

An unambiguous finding at reconstructed NMJs was that a large and variable fraction (about one-half) of boutons contributed no synaptic current, even in the "good fit" configuration. The culprit was probably misalignment, because all boutons took up activity-dependent probes. This represents a serious limitation of the reconstruction technique, namely, that the number of active boutons, and therefore quantal content and MEPP frequency, is unpredictable. Thus, these important measurable quantities cannot be meaningfully compared among "mixed" reconstructed NMJs in the same manner as MEPP amplitudes. One approach toward overcoming this limitation, which we are now pursuing, is formation of reconstructed NMJs that comprise a single bouton applied to an endplate site.

References

Balice-Gordon RJ, Breedlove SM, Bernstein S, Lichtman JW (1990) Neuromuscular junctions shrink and expand as muscle fiber size is manipulated: *in vivo* observations in the androgen-sensitive bulbocavernosus muscle of mice. J Neurosci 10:2660–2671.

Bartol TM Jr, Land BR, Salpeter EE, Salpeter MM (1991) Monte Carlo simulation of miniature endplate current generation in the vertebrate neuromuscular junction. Biophys J 59:1290–1307.

Betz W, Sakmann B (1973) Effects of proteolytic enzymes on function and structure of frog neuromuscular junctions. J Physiol (Lond) 230: 673–688.

Betz WJ, Mao F, Bewick GS (1992) Activity-dependent fluorescent staining and destaining of living vertebrate motor nerve terminals. J Neurosci 12:363–375.

Bowman WC, Marshall IG, Gibb AJ, Harborne AJ (1988) Feedback control of transmitter release at the neuromuscular junction. Trends Pharmacol Sci 9:16–20.

Coniglio LM, Hardwick JC, Parsons RL (1993) Quantal transmitter release at snake twitch and tonic muscle fibers during prolonged never terminal depolarization. J Physiol (Lond) 466:383–403.

Dionne VE, Leibowitz MD (1982) Acetylcholine receptor kinetics: a description from single-channel currents at snake neuromuscular junctions. Biophys J 39:253–261.

Drewe JA, Childs GV, Kunze DL (1988) Synaptic transmission between dissociated adult mammalian neurons and attached synaptic boutons. Science 241:1810–1813.

Fazeli MS (1992) Synaptic plasticity: on the trail of the retrograde messenger. Trends Neurosci 15:115–117.

Girod R, Poo MM, Colli LE, Medilanski J, Ofori S, Dunant Y (1990) Acetylcholine release by isolated nerve terminals (synaptosomes) is quantal. Soc Neurosci Abstr 16:167.

Grinnell AD, Herrera AA (1981) Specificity and plasticity of neuromuscular connections: long term regulation of motoneuron function. Prog Neurobiol 17:203–282.

Hall ZW, Kelly RB (1971) Enzymatic detachment of endplate acetylcholinesterase from muscle. Nature New Biol 232:62–63.

Harris JB, Ribchester RR (1979) The relation between end-plate size and transmitter release in normal and dystrophic muscles of the mouse. J Physiol (Lond) 296:245–265.

Herrera AA, Banner LR (1990) The use and effects of vital fluorescent dyes: observation of motor nerve terminals and satellite cells in living frog muscles. J Neurocytol 19:67–83.

Katz B, Miledi R (1973) The binding of acetylcholine to receptors and its removal from the synaptic cleft. J Physiol (Lond) 231:549–574.

Ko C-P, Folsom DB (1989) Induction of active zones at ectopic neuromuscular junctions in the frog. J Neurosci 9:3392–3399.

Korn H, Faber DS (1991) Quantal analysis and synaptic efficacy in the CNS. Trends Neurosci 14:439–444.

Korn H, Mallet A, Triller A, Faber DS (1982) Transmission at a central inhibitory synapse. II. Quantal description of release, with a physical correlate for binomial *n*. J Neurophysiol 48:679–707.

Kuffler SW, Yoshikami D (1975) The distribution of acetylcholine sensitivity at the post-synaptic membrane of vertebrate skeletal twitch muscle: iontophoretic mapping in the micron range. J Physiol (Lond) 244:703–730.

Kuno M, Turkanis SA, Weakly JN (1971) Correlation between nerve terminal size and transmitter release at the neuromuscular junction of the frog. J Physiol (Lond) 213:545–556.

Lichtman JW, Wilkinson RS (1987) Properties of motor units in the transversus abdominis muscle of the garter snake. J Physiol (Lond) 393:355–374.

Lichtman JW, Wilkinson RS, Rich MM (1985) Multiple innervation of tonic endplates revealed by activity-dependent uptake of fluorescent probes. Nature 314:357–359.

Lichtman JW, Sunderland W, Wilkinson RS (1989) High resolution imaging of synaptic structure with a simple confocal microscope. New Biol 1:75–82.

Magrassi L, Purves D, Lichtman JW (1987) Fluorescent probes that stain living nerve terminals. J Neurosci 7:1207–1214.

McMahan UG, Spitzer NC, Pepper K (1972) Visual identification of nerve terminals in living isolated skeletal muscle. Proc R Soc Lond [Biol] 181:421–430.

Neher E, Sakman B, Steinbach JH (1978) The extracellular patch clamp: a method for resolving currents through individual open channels in biological membranes. Pfluegers Arch 375:219–228.

Nemeth PM, Rosser BWC, Wilkinson RS (1991) Metabolic and contractile uniformity of isolated motor unit fibres of snake muscle. J Physiol (Lond) 434:41–55.

Nudell BM, Grinnell AD (1982) Inverse relationship between transmitter release and terminal length in synapses on frog muscle fibers of uniform input resistance. J Neurosci 2:216–224.

Nystrom RR, Ko C-P (1988) Disruption of active zones in frog neuromuscular junctions following treatment with proteolytic enzymes. J Neurocytol 17:63–71.

Propst JW, Ko C-P (1987) Correlations between active zone ultrastructure and synaptic function studied with freeze-fracture of physiologically identified neuromuscular junctions. J Neurosci 7:3654–3664.

Ridge RMAP (1971) Different types of extrafusal muscle fibres in snake costocutaneous muscle. J Physiol (Lond) 217:393–418.

Smith DO (1991) Sources of adenosine released during neuromuscular transmission in the rat. J Physiol (Lond) 432:343–354.

Trube G (1983) Enzymat' dispersion of heart and other tissues. In: Single-channel recording (Sakman B, Neher E, eds), pp 69–76. New York: Plenum.

Van der Kloot W (1991) The regulation of quantal size. Prog Neurobiol 36:93–130.

Vautrin J, Mambrini J (1989) Synaptic current between neuromuscular junction folds. J Theor Biol 140:479–498.

Walrond JP, Reese TS (1985) Structure of axon terminals and active zones at synapses on lizard twitch and tonic muscle fibers. J Neurosci 5:1118–1131.

Wilkinson RS (1988) Quantal release from identified synaptic boutons in snake muscle. Soc Neurosci Abstr 14:108.

Wilkinson RS, Lichtman JW (1985) Regular alternation of fiber types in the transversus abdominis muscle of the garter snake. J Neurosci 5:2979–2988.

Wilkinson RS, Lunin SD (1991) Enzymatically dissociated NMJs function almost normally after manual reattachment of terminal to endplate. Soc Neurosci Abstr 17:1332.

Wilkinson RS, Lunin SD (1992) Isolated snake neuromuscular boutons release 2–3 quanta when activated. Soc Neurosci Abstr 18:1340.

Wilkinson RS, Nemeth PM (1989) Metabolic fiber types of snake transversus abdominis muscle. Am J Physiol 256:C1176–C1183.

Wilkinson RS, Rosser BWC, Nemeth PM, Sweeney HL (1991) Metabolic capacity and myosin expression in single muscle fibres of the garter snake. J Physiol (Lond) 440:113–129.

Wilkinson RS, Lunin SD, Stevermer JJ (1992) Regulation of single quantal efficacy at the snake neuromuscular junction. J Physiol (Lond) 448:413–436.